

# Platinum(II) 2,4-Di(2'-pyridyl)-6-(*p*-tolyl)-1,3,5-triazine Complexes: Synthesis and Photophysics

Pin Shao, Yunjing Li, and Wenfang Sun\*

Department of Chemistry and Molecular Biology, North Dakota State University,  
Fargo, North Dakota 58105-5516

Received December 23, 2007

Five platinum(II) complexes based on the 2,4-di(2'-pyridyl)-6-(*p*-tolyl)-1,3,5-triazine ligand (**1–5**) have been synthesized and characterized. The effects of the triazine-containing terdentate ligand on the photophysics and nonlinear transmission have been explored. The influence of the monodentate ligand, i.e. chloride, pentynyl, and phenylacetylide, and counteranion on the photophysical and nonlinear transmission characteristics of these complexes has also been systematically investigated. It is found that, due to the electron-deficient nature of the triazine ring and the extension of the  $\pi$  system between the terdentate ligand and the 6-(*p*-tolyl) substituent, the metal-to-ligand charge transfer (MLCT) bands in both the UV–vis spectra ( $^1\text{MLCT}$ ) and the emission spectra ( $^3\text{MLCT}$ ) red-shift in comparison to those of the corresponding platinum(II) complexes with 2,2':6',2''-terpyridyl ligands. However, both the emission efficiency from the  $^3\text{MLCT}$  state and the emission lifetime are significantly reduced. The different monodentate ligands cause a decrease of the energy of the  $^1\text{MLCT}$  band, going down from the complex with a chloride ligand (**1** and **2**) to **3** and **4** with a pentynyl ligand to **5** with a phenylacetylide ligand. The chloride-containing complex (**2**) only shows a terdentate ligand  $^1\pi,\pi^*$  originated emission at 460 nm, while the pentynyl-containing complexes (**3** and **4**) exhibit an  $^3\text{MLCT}$ -based emission at  $\sim 615$  nm with a lifetime of approximately 180 ns. In contrast, complex **5** with the phenylacetylide ligand emits at both 460 and 622 nm. Among these five complexes, only **3** and **4** exhibit a moderate triplet transient absorption, with a positive band extending from 510 to 820 nm. The lifetimes of the transients are approximately 200 ns, which is tentatively assigned to the  $^3\text{MLCT}$  excited state. Complexes **3–5** display a weak nonlinear transmission that is affected by the monodentate ligand and the counteranions. In addition, it is revealed that the counteranion has a negligible effect on the  $^1\text{MLCT}$  state, whereas its effect on the  $^3\text{MLCT}$  state is drastic, especially on the triplet excited-state absorption coefficient, the quantum yield of the triplet state formation, the quantum yield of the  $^3\text{MLCT}$  emission, and the nonlinear transmission, as exemplified by complexes **3** and **4**.

## Introduction

Platinum(II) terpyridyl complexes have attracted a great deal of interest in recent years due to their versatile potential applications in chemical sensors,<sup>1</sup> organic light-emitting devices (OLED),<sup>2</sup> nonlinear transmission devices,<sup>3</sup> DNA intercalation

and protein probes,<sup>4</sup> and dye-sensitized solar cells.<sup>5</sup> All these applications are based on their square-planar configuration and unique spectroscopic properties. Photophysical studies have revealed that the nature of the low-lying charge transfer (CT) band of the platinum terpyridyl complexes has a great effect on their optical properties.<sup>6</sup> Recent theoretical studies on some amino-containing platinum(II) terpyridyl complexes indicated that the low-lying CT band could be ascribed to a metal-to-ligand charge-transfer (MLCT) transition mixed with some ligand-to-ligand charge-transfer (LLCT) transition.<sup>7</sup> In both cases, the lowest unoccupied molecular orbital (LUMO) is

\* To whom correspondence should be addressed. E-mail: Wenfang.Sun@ndsu.edu.

(1) (a) Yang, Q.-Z.; Wu, L.-Z.; Zhang, H.; Chen, B.; Wu, Z.-X.; Zhang, L.-P.; Tung, Z.-H. *Inorg. Chem.* **2004**, *43*, 5195. (b) Wu, L. Z.; Cheung, T. C.; Che, C. M.; Cheung, K. K.; Lam, M. H. W. *Chem. Commun.* **1998**, *10*, 1127. (c) Wong, K.-H.; Chan, M. C.-W.; Che, C. M. *Chem. Eur. J.* **1999**, *5*, 2845. (d) Kui, S. C. F.; Chui, S. S.-Y.; Che, C.-M.; Zhu, N. *J. Am. Chem. Soc.* **2006**, *128*, 8297.

(2) (a) Lu, W.; Mi, B. X.; Chan, M. C. W.; Hui, Z.; Che, C. M.; Zhu, N.; Lee, S. T. *J. Am. Chem. Soc.* **2004**, *126*, 4958. (b) Yesin, H.; Donges, D.; Humbs, W.; Strasser, J.; Sitters, R.; Glasbeek, M. *Inorg. Chem.* **2002**, *41*, 4915. (c) Brooks, J.; Babayan, Y.; Lamansky, S.; Djurovich, P. I.; Tsyba, I.; Bau, R.; Thompson, M. E. *Inorg. Chem.* **2002**, *41*, 3055. (d) Shi, J. C.; Chao, H. Y.; Fu, W. F.; Peng, S. M.; Che, C. M. *Dalton Trans.* **2000**, *18*, 3128. (e) Chassot, L.; von Zelewsky, A.; Sandrini, D.; Maestri, M.; Balzani, V. *J. Am. Chem. Soc.* **1986**, *108*, 6084. (f) Maestri, M.; Sandrini, D.; Balzani, V.; Chassot, L.; Jolliet, P.; von Zelewsky, A. *Chem. Phys. Lett.* **1985**, *122*, 375. (g) Wong, W.-Y.; He, Z.; So, S.-K.; Tong, K.-L.; Lin, Z. *Organometallics* **2005**, *24*, 4079. (h) He, Z.; Wong, W.-Y.; Yu, X.; Kwok, H.-S.; Lin, Z. *Inorg. Chem.* **2006**, *45*, 10922.

(3) (a) Sun, W.; Wu, Z.-X.; Yang, Q.-Z.; Wu, L.-Z.; Tung, C.-H. *Appl. Phys. Lett.* **2003**, *82*, 850. (b) Guo, F.; Sun, W.; Liu, Y.; Schanze, K. *Inorg. Chem.* **2005**, *44*, 4055. (c) Sun, W.; Guo, F. *Chin. Opt. Lett.* **2005**, *S3*, S34. (d) Guo, F.; Sun, W. *J. Phys. Chem. B* **2006**, *110* (30), 15029.

(4) (a) Lippard, S. J. *Acc. Chem. Res.* **1978**, *11*, 211. (b) Arena, G.; Monsú Scolaro, L.; Pasternack, R. F.; Romeo, R. *Inorg. Chem.* **1995**, *34*, 2994. (c) Ratilla, E. M. A.; Brothers, H. M., II.; Kostić, N. M. *J. Am. Chem. Soc.* **1987**, *109*, 4592.

(5) (a) Wadas, T. J.; Chakraborty, S.; Lachicotte, R. J.; Wang, Q.-M.; Eisenberg, R. *Inorg. Chem.* **2005**, *44*, 2628. (b) Chakraborty, S.; Wadas, T. J.; Hester, H.; Flaschenreim, C.; Schmehl, R.; Eisenberg, R. *Inorg. Chem.* **2005**, *44*, 6865.

(6) (a) Michalec, J. F.; Bejune, S. A.; Cuttall, D. G.; Summerton, G. C.; Gertenbach, J. A.; Field, J. S.; Haines, R. J.; McMillin, D. R. *Inorg. Chem.* **2001**, *40*, 2193. (b) Crites, D. K.; Cunningham, C. T.; McMilin, D. R. *Chim. Acta* **1998**, *273*, 346.

(7) (a) Zhou, X.; Zhang, H.-X.; Pan, Q.-J.; Xia, B.-H.; Tang, A.-C. *J. Phys. Chem. A* **2005**, *109*, 8809. (b) Liu, X.-J.; Feng, J.-K.; Meng, J.; Pan, Q.-J.; Ren, A.-M.; Zho, X.; Zhang, H.-X. *Eur. J. Inorg. Chem.* **2005**, 1856. (c) Hua, F.; Kinayyigit, S.; Cable, J. R.; Castellano, F. N. *Inorg. Chem.* **2006**, *45*, 4304.

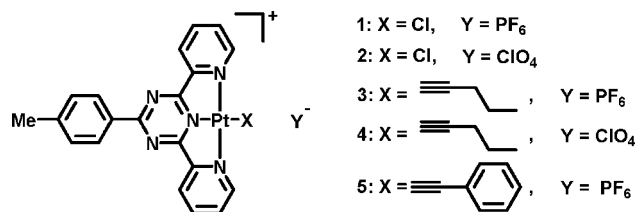


**Figure 1.** Structures of platinum(II) 2,4-di(2'-pyridyl)-6-(p-tolyl)-1,3,5-triazine complexes.

located on the terpyridyl ring. Thus, both the absorption and the emission bands associated with the CT transition(s) could be tuned by modification of the terpyridyl ligand.<sup>3d,6,8</sup> In general, introducing electron-withdrawing substituents (–CN, –NO<sub>2</sub>, etc.) on the 4'-position of the terpyridyl ligand or extending the conjugation of the terpyridyl ligand by incorporating a 4'-aryl substituent on the terpyridyl ligand can stabilize the LUMO.<sup>6</sup> As a result, the low-lying CT band(s) will red-shift. However, the effect of expanding the conjugation by the 4'-aryl substituent(s) is usually limited, because the unfavorable repulsive interactions between the hydrogens adjacent to the interannular bond cause the 4'-aryl substituent to twist out of the terpyridyl plane, which reduces the  $\pi$ -orbital overlap between the aryl substituent and the terpyridyl rings. To remove the unfavorable repulsive interactions, Hanan and co-workers replaced the central pyridine ring with a triazine ring or used the 4'-(2-pyrimidyl) substituent instead of the 4'-phenyl substituent and investigated the photophysics of the corresponding Ru(II) and Zn(II) complexes.<sup>9</sup> The crystal structures of the Ru complexes have revealed that the 4'-aryl substituent lies almost coplanar with the terdentate ligand.<sup>9a-d</sup> The MLCT band energy is thus reduced, showing a red shift in the absorption and the emission spectra and an increased emission lifetime. In addition, Fe, Co, Ni, and Cu complexes based on the 2,4-di(2'-pyridyl)-1,3,5-triazine ligand have also been reported by this group.<sup>10</sup> However, to date, no platinum(II) complexes have been reported based on this approach. To remedy this deficiency, our group recently synthesized a series of platinum(II) complexes (Figure 1) containing the 2,4-di(2'-pyridyl)-6-(p-tolyl)-1,3,5-triazine ligand (**L**) and investigated their photophysical properties and nonlinear transmission behavior. Different monodentate ligands (chloride, pentynyl, and phenylacetylide) and different counteranions (ClO<sub>4</sub><sup>−</sup> and PF<sub>6</sub><sup>−</sup>) are used to study the effect of the monodentate ligand and the counteranion on the photophysics of these platinum(II) complexes.

## Experimental Section

**Synthesis.** The ligand 2,4-di(2'-pyridyl)-6-(p-tolyl)-1,3,5-triazine (**L**) was synthesized according to the reported procedure.<sup>9b</sup> All the

starting chemicals were purchased from Alfa Aesar, and the solvents were used as received unless otherwise stated.

<sup>1</sup>H NMR spectra were measured on a Varian 300 MHz VNMR spectrometer. ESI-HRMS analyses were conducted on a Bruker Daltonics BioTOF III mass spectrometer. Elemental analyses were conducted by NuMega Resonance Laboratories, Inc., San Diego, CA.

**Complex 1.** A 0.163 g portion of **L** and 0.208 g of K<sub>2</sub>PtCl<sub>4</sub> were refluxed in 30 mL of acetonitrile/H<sub>2</sub>O (1/1, v/v) for 24 h. The volume of the reaction mixture was then reduced to ~10 mL, and the precipitates were collected. The solid was dissolved in a small amount of DMF, and this solution was filtered into a saturated NH<sub>4</sub>PF<sub>6</sub> aqueous solution. The mixture was then stirred overnight at room temperature. The yellow-brown precipitates were filtered out, washed with water and ether, and dried in a vacuum oven. Yield: 41%. <sup>1</sup>H NMR (DMSO-*d*<sub>6</sub>):  $\delta$  9.14 (d, *J* = 4.5 Hz, 2H), 8.94 (d, *J* = 7.5 Hz, 2H), 8.76 (d, *J* = 8.1 Hz, 2H), 8.70 (td, *J* = 1.5 and 7.8 Hz, 2H), 8.25 (t, *J* = 6.6 Hz, 2H), 7.57 (d, *J* = 8.4 Hz, 2H), 2.48 (s, 3H) ppm. ESI-MS: *m/z* calcd for [C<sub>20</sub>ClH<sub>15</sub>N<sub>5</sub>Pt<sup>194</sup>]<sup>+</sup> 555.0660, found 554.9987 (97%); *m/z* calcd for [C<sub>20</sub>ClH<sub>15</sub>N<sub>5</sub>Pt<sup>195</sup>]<sup>+</sup> 556.0653, found 555.9980 (100%); *m/z* calcd for [C<sub>20</sub>ClH<sub>15</sub>N<sub>5</sub>Pt<sup>196</sup>]<sup>+</sup> 557.0652, found 556.9972 (47%). Anal. Calcd for C<sub>20</sub>H<sub>15</sub>ClF<sub>6</sub>N<sub>5</sub>Pt: C, 34.27; H, 2.16; N, 9.99. Found: C, 34.27; H, 1.96; N, 10.23.

**Complex 2.** The procedure was similar to that for the synthesis of **1**, except Mg(ClO<sub>4</sub>)<sub>2</sub> was used instead of NH<sub>4</sub>PF<sub>6</sub>. Yield: 46%. <sup>1</sup>H NMR (DMSO-*d*<sub>6</sub>):  $\delta$  9.11 (d, *J* = 5.4 Hz, 2H), 8.94 (d, *J* = 7.5 Hz, 2H), 8.76 (d, *J* = 8.1 Hz, 2H), 8.70 (t, *J* = 8.1 Hz, 2H), 8.23 (t, *J* = 6.6 Hz, 2H), 7.56 (d, *J* = 8.7 Hz, 2H), 2.49 (s, 3H) ppm. ESI-MS: *m/z* calcd for [C<sub>20</sub>ClH<sub>15</sub>N<sub>5</sub>Pt<sup>194</sup>]<sup>+</sup> 555.0660, found 555.1128 (94%); *m/z* calcd for [C<sub>20</sub>ClH<sub>15</sub>N<sub>5</sub>Pt<sup>195</sup>]<sup>+</sup> 556.0653, found 556.1108 (100%); *m/z* calcd for [C<sub>20</sub>ClH<sub>15</sub>N<sub>5</sub>Pt<sup>196</sup>]<sup>+</sup> 557.0652, found 557.1110 (46%). Anal. Calcd for C<sub>20</sub>H<sub>15</sub>Cl<sub>2</sub>N<sub>5</sub>O<sub>4</sub>Pt: C, 36.65; H, 2.31; N, 10.69. Found: C, 36.91; H, 2.70; N, 10.89.

**Complex 3.** A mixture of 30 mg of KOH in 200 mL of methanol was purged with argon for 30 min. Then 40  $\mu$ L of pentyne was added, and the mixture was stirred for 30 min under an argon atmosphere. A 100 mg portion of **1** and 5 mg of CuI were added. The mixture was continuously stirred under argon at room temperature for 48 h. After that, the solvent was removed under reduced pressure. The residue was extracted with dichloromethane and dried over anhydrous Na<sub>2</sub>SO<sub>4</sub>. The crude product was purified by passing through a short silica column twice; dichloromethane/acetone (20/1, v/v) was used as the eluent. The product was further purified by recrystallization from dichloromethane and ether. Yield: 2%. <sup>1</sup>H NMR (CD<sub>3</sub>CN):  $\delta$  9.08 (d, *J* = 4.5 Hz, 2H), 8.74 (m, 4H), 8.51 (t, *J* = 8.1 Hz, 2H), 7.94 (br, s, 2H), 7.56 (d, *J* = 7.5 Hz, 2H), 2.54 (s, 3H), 2.48 (t, *J* = 7.5 Hz, 2H), 1.59 (q, *J* = 7.2 Hz, 2H), 1.02 (t, *J* = 7.2 Hz, 3H) ppm. ESI-MS: *m/z* calcd for [C<sub>25</sub>H<sub>22</sub>N<sub>5</sub>Pt<sup>194</sup>]<sup>+</sup> 586.1496, found 586.0775 (74%); *m/z* calcd for [C<sub>25</sub>H<sub>22</sub>N<sub>5</sub>Pt<sup>195</sup>]<sup>+</sup> 587.1519, found 587.0801 (100%); *m/z* calcd for [C<sub>25</sub>H<sub>22</sub>N<sub>5</sub>Pt<sup>196</sup>]<sup>+</sup> 588.1528, found 588.0822 (84%). Anal. Calcd for C<sub>25</sub>H<sub>22</sub>F<sub>6</sub>N<sub>5</sub>Pt • 1.8CH<sub>2</sub>Cl<sub>2</sub>: C, 36.36; H, 2.91; N, 7.91. Found: C, 36.47; H, 3.38; N, 7.55.

**Complex 4.** The procedure was similar to that for the synthesis of **3**, except **2** was used instead of **1**. Yield: 7%. <sup>1</sup>H NMR (CD<sub>3</sub>CN):  $\delta$  9.18 (br s, 2H), 8.70 (m, 4H), 8.51 (br s, 2H), 7.99 (br s, 2H), 7.53 (d, *J* = 6.9 Hz, 2H), 2.53 (s, 3H), 2.46 (m, 2H), 1.65 (m, 2H), 1.09 (t, *J* = 7.8 Hz, 3H) ppm. ESI-MS: *m/z* calcd for [C<sub>25</sub>H<sub>22</sub>N<sub>5</sub>Pt<sup>194</sup>]<sup>+</sup> 586.1496, found 586.1909 (76%); *m/z* calcd for [C<sub>25</sub>H<sub>22</sub>N<sub>5</sub>Pt<sup>195</sup>]<sup>+</sup> 587.1519, found 587.1937 (100%); *m/z* calcd for [C<sub>25</sub>H<sub>22</sub>N<sub>5</sub>Pt<sup>196</sup>]<sup>+</sup> 588.1528, found 588.1961 (81%). Anal. Calcd for C<sub>25</sub>H<sub>22</sub>N<sub>5</sub>ClO<sub>4</sub>Pt • 0.8CH<sub>2</sub>Cl<sub>2</sub>: C, 41.05; H, 3.15; N, 9.28. Found: C, 40.99; H, 3.23; N, 8.96.

**Complex 5.** A mixture of 30 mg of KOH in 5 mL of DMF was purged with argon for 30 min, and then 20  $\mu$ L of phenylacetylene was added and the mixture was stirred for 30 min. A 120 mg portion

(8) (a) Michalec, J. F.; Bejune, S. A.; McMillin, D. R. *Inorg. Chem.* **2000**, *39*, 2708. (b) Chakraborty, S.; Wadas, T. J.; Hester, H.; Flaschenreim, C.; Schmehl, R.; Eisenberg, R. *Inorg. Chem.* **2005**, *44*, 6284. (c) Crites, D. K.; Cunningham, C. T.; McMillin, D. R. *Inorg. Chim. Acta* **1998**, *273*, 346.

(9) (a) Polson, M. I. J.; Taylor, N. J.; Hanan, G. S. *Chem. Commun.* **2002**, 1356. (b) Polson, M. I. J.; Medlycott, E. A.; Hanan, G. S.; Mikelsons, L.; Taylor, N. J.; Watanabe, M.; Tanaka, Y.; Loiseau, F.; Passalacqua, R.; Campagna, S. *Chem. Eur. J.* **2004**, *10*, 3640. (c) Medlycott, E. A.; Hanan, G. S. *Inorg. Chem. Commun.* **2007**, *10*, 229. (d) Fang, Y.-Q.; Taylor, N. J.; Laverdiere, F.; Hanan, G. S.; Loiseau, F.; Nastasi, F.; Campagna, S.; Nierengarten, H.; Leize-Wagner, E.; Dorsselaer, A. V. *Inorg. Chem.* **2007**, *46*, 2854. (e) Medlycott, E. A.; Hanan, G. S. *Coord. Chem. Rev.* **2006**, *250*, 1763.

(10) Medlycott, E. A.; Udachin, K. A.; Hanan, G. S. *Dalton Trans.* **2007**, 430.

of **1** and 8 mg of CuI were added. After the mixture was stirred under argon at room temperature for 24 h, the reaction mixture was filtered and 50 mL of ether was added to the filtrate. The precipitates were then collected and purified twice by recrystallization in acetonitrile and ether. A brown-red solid was obtained (yield 57%).  $^1\text{H NMR}$  (DMSO- $d_6$ ):  $\delta$  9.22 (s, 2H), 8.84 (d,  $J = 7.2$  Hz, 2H), 8.64 (m, 4H), 8.12 (s, 2H), 7.49 (t,  $J = 9.2$  Hz, 4H), 7.31 (t,  $J = 7.2$  Hz, 2H), 7.23 (t,  $J = 7.2$  Hz, 1H), 2.46 (s, 3H) ppm. ESI-MS:  $m/z$  calcd for  $[\text{C}_{28}\text{H}_{20}\text{N}_5\text{Pt}^{194}]^+$  620.1340, found 620.2302 (75%);  $m/z$  calcd for  $[\text{C}_{28}\text{H}_{20}\text{N}_5\text{Pt}^{195}]^+$  621.1363, found 621.2326 (100%);  $m/z$  calcd for  $[\text{C}_{28}\text{H}_{20}\text{N}_5\text{Pt}^{196}]^+$  622.1373, found 622.2340 (86%). Anal. Calcd for  $\text{C}_{28}\text{H}_{20}\text{N}_5\text{PtPF}_6$ : C, 43.87; H, 2.63; N, 9.14. Found: C, 43.84; H, 2.65; N, 9.54.

**Photophysical Measurements.** The UV-vis absorption spectra were measured on an Agilent 8453 spectrophotometer. Dichloromethane was used as the solvent. The steady-state emission spectra were obtained on a SPEX Fluorolog-3 fluorometer/phosphorometer. The emission quantum yields of the samples were determined by a comparative method,<sup>11</sup> in which a degassed aqueous solution of  $[\text{Ru}(\text{bpy})_3]\text{Cl}_2$  ( $\Phi_{\text{em}} = 0.042$ , excited at 436 nm)<sup>12</sup> was used as the reference. The emission lifetimes and the triplet transient difference absorption spectra were measured on an Edinburgh LP920 laser flash photolysis spectrometer. The third harmonic output (355 nm) of a Nd:YAG laser (Quantel Brilliant, pulse width (fwhm)  $\sim 4.1$  ns, repetition rate 10 Hz) was used as the excitation source. The laser repetition rate was set to 1 Hz, and the output energy at 355 nm was adjusted to  $\sim 5$  mJ/pulse. Each sample was purged with argon for 30 min before measurement.

The triplet excited-state molar extinction coefficient and triplet quantum yield were determined by the partial saturation method.<sup>13</sup> The optical density at 705 nm was monitored when the excitation energy at 355 nm was gradually increased. Saturation was observed when the excitation energy was higher than 3.6 mJ for **3** and 5.5 mJ for **4**. The following equation was then used to fit the experimental data to obtain  $\epsilon_T$  and  $\Phi_T$ :<sup>13</sup>

$$\Delta\text{OD} = \alpha(1 - \exp(-bI_p)) \quad (1)$$

where  $\Delta\text{OD}$  is the optical density change at 705 nm,  $I_p$  is the pump intensity in einstein  $\text{cm}^{-2}$ ,  $a = (\epsilon_T - \epsilon_0)dl$ , and  $b = 2303\epsilon_0^{\text{ex}}\Phi_T/A$ .  $\epsilon_T$  and  $\epsilon_0$  are the absorption coefficients of the excited state and the ground state at 705 nm,  $\epsilon_0^{\text{ex}}$  is the ground-state absorption coefficient at the excitation wavelength of 355 nm,  $d$  is the concentration of the sample ( $\text{mol L}^{-1}$ ),  $l$  is the thickness of the sample excited by the excitation beam (namely the diameter of the excitation beam), and  $A$  is the area of the sample irradiated by the excitation beam. The concentration used for this experiment was  $3.0 \times 10^{-5}$  mol  $\text{L}^{-1}$  for **3** and  $2.9 \times 10^{-5}$  mol  $\text{L}^{-1}$  for **4**.

**Nonlinear Transmission Measurements.** The nonlinear transmission measurements were conducted using a setup that has been described previously.<sup>3b,c</sup> A Quantel Brilliant Nd:YAG laser was used as the light source and was operated at its second-harmonic output (532 nm) with a 10 Hz repetition rate.

## Results and Discussion

**Electronic Absorption Spectra.** Figure 2 shows the electronic absorption spectra of complexes **1–5** in dichloromethane ( $\text{CH}_2\text{Cl}_2$ ). All these complexes exhibit strong absorbing bands below 400 nm, which could be assigned to the  $^1\pi,\pi^*$  transitions within the 2,4-di(2'-pyridyl)-6-(*p*-tolyl)-1,3,5-triazine ligand. The broad bands from 400 to 600 nm most likely arise from the

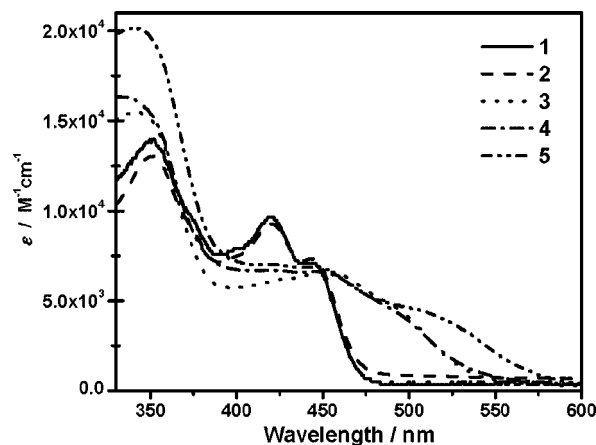


**Figure 2.** Electronic absorption spectra of complexes **1–5** in  $\text{CH}_2\text{Cl}_2$ .

metal-to-ligand charge transfer ( $^1\text{MLCT}$ ) transitions, which have been reported in many other platinum(II) terpyridyl complexes (Table 1).<sup>3b,6,7,14</sup> For complexes **1** and **2**, the MLCT band maximum is located at  $\sim 420$  nm, with a shoulder appearing at  $\sim 450$  nm. In contrast, the MLCT bands of their corresponding acetylide complexes **3–5** become broader and red-shift to 450 nm. Especially for complex **5**, there is an additional shoulder appearing at ca. 512 nm, which indicates that there might be two orbitally distinct MLCT transitions, e.g.,  $d_{xz}(\text{Pt}) \rightarrow \pi^*(\text{L})$  and  $d_{yz}(\text{Pt}) \rightarrow \pi^*(\text{L})$  (assuming that the acetylide ligand is along the  $x$  axis with  $z$  perpendicular to the coordination plane). This is consistent with what has been observed in platinum(II) terpyridyl acetylide complexes<sup>1a,3b</sup> and diimine platinum(II) bis-acetylide complexes.<sup>15</sup> The red shift of the  $^1\text{MLCT}$  band in complexes **3–5** in comparison to the bands in **1** and **2** can be explained by the fact that the HOMOs of the platinum complexes are predominantly metal-based and the energy of the HOMOs could be modulated by the auxiliary ligand(s). The strong electron-donating ability of the acetylide ligand(s) would destabilize the HOMO(s), thus leading to a decrease of the energy gap between the metal-based HOMO and the terdentate ligand-based LUMO. On comparison of the absorption spectra of the platinum 4'-tolylterpyridyl analogues<sup>3b</sup> to those of complexes **1–5**, it is quite obvious that the  $^1\text{MLCT}$  bands of **1–5** are broader and more red-shifted. For example, the  $^1\text{MLCT}$  band of **4** extends to 550 nm, while its 4'-tolylterpyridyl analogue shows almost no absorption beyond 500 nm.<sup>16</sup> Complex **5** exhibits a moderate absorption from 500 to 600 nm, while its 4'-tolylterpyridyl analogue is transparent above 550 nm.<sup>3b</sup> This red shift can be attributed to the following two factors: (1) the  $\pi^*$  orbital of the triazine-containing terdentate ligand is lower than that of the 4'-tolylterpyridyl ligand due to the electron-deficient nature of the triazine ring, and (2) the unfavorable repulsive interactions between the hydrogens adjacent to the interannular bond have been removed in the triazine-based ligand, which yields an almost coplanar configuration between the tolyl substituent and the terdentate ligand.

(14) (a) Wong, K. M.-C.; Tang, W.-S.; Chu, B. W.-K.; Zhu, N.; Yam, V. W.-W. *Organometallics* **2004**, *23*, 3459. (b) Shikhova, E.; Danilov, E. O.; Kinayigit, S.; Pomestchenko, I. E.; Tregubov, A. D.; Camerel, F.; Retaileau, P.; Ziessel, R.; Castellano, F. N. *Inorg. Chem.* **2007**, *46*, 3038. (c) Yam, V. W.-W.; Tang, R. P.-L.; Wong, K. M.-C.; Cheung, K.-K. *Organometallics* **2001**, *20*, 4476.

(15) Whittle, C. E.; Weinstein, J. A.; George, M. W.; Schanze, K. S. *Inorg. Chem.* **2001**, *40*, 4053.

(16) Yang, Q.-Z.; Wu, L.-Z.; Wu, Z.-X.; Zhang, L.-P.; Tung, C.-H. *Inorg. Chem.* **2002**, *41*, 5653.

(11) Demas, J. N.; Crosby, G. A. *J. Phys. Chem.* **1971**, *75*, 991.

(12) van Houten, J.; Watts, R. J. *J. Am. Chem. Soc.* **1976**, *98*, 4853.

(13) (a) Carmichael, I.; Hug, G. L. *J. Phys. Chem. Ref. Data* **1986**, *15*, 1. (b) Schermann, G.; Schmidt, R.; Völcker, A.; Brauer, H.-D.; Mertes, H.; Franck, B. *Photochem. Photobiol.* **1990**, *52*, 741.

**Table 1. Photophysical Parameters of Complexes 1–5 at Room Temperature**

Complex	$\lambda_{\text{abs}}/\text{nm}$ ( $\epsilon/\text{M}^{-1} \cdot \text{cm}^{-1}$ ) <sup>d</sup>	$\lambda_{\text{em}}/\text{nm}$ ( $\tau_{\text{em}}/\text{ns}$ ); <sup>d</sup> $\Phi_{\text{em}}$	$\tau_{\text{TA}}/\text{ns}$ <sup>e</sup>
<b>1</b> <sup>a</sup>	277 (26 400), 330 (16 600), 408 (7550), 428 (6350)		
<b>2</b> <sup>b</sup>	271 (21 300), 300 (25 800), 313 (22 700), 335 (22 400), 406 (11 700), 426 (9100)	460	
<b>3</b> <sup>c</sup>	285 (21 400), 303 (20 900), 342 (15 400), 423 (6250), 455 (6650)	614 (183);0.0007	224
<b>4</b> <sup>c</sup>	283 (24 600), 303 (22 800), 339 (16 200), 422 (6710), 448 (6630)	616 (178);0.0018	177
<b>5</b> <sup>b</sup>	250 (36 700), 260 (36 000), 290 (31 200), 328 (20 300), 424 (6100), 467 (4900)	460, 622	

<sup>a</sup> DMF was used as solvent. <sup>b</sup> Acetonitrile was used as solvent. <sup>c</sup> CH<sub>2</sub>Cl<sub>2</sub> was used as solvent. <sup>d</sup> Measured at a concentration of  $\sim 10^{-5}$  M. <sup>e</sup> Monitored at 705 nm.

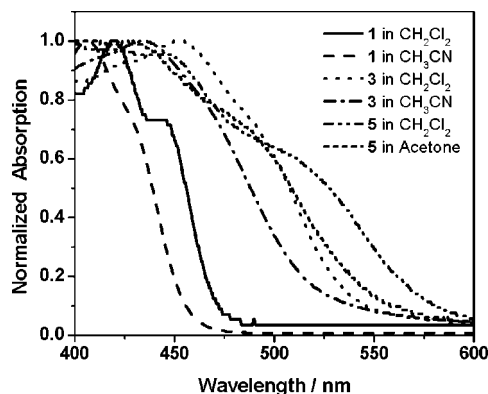


**Figure 3.** Electronic absorption spectra of complexes **1**, **3**, and **5** in CH<sub>2</sub>Cl<sub>2</sub> and CH<sub>3</sub>CN (**5** is in acetone).

As a result, the  $\pi$  system of the terdentate ligand is extended, which further reduces the energy of the  $\pi^*$  orbital.

The solvent-dependent study in CH<sub>2</sub>Cl<sub>2</sub> and CH<sub>3</sub>CN (acetone was used for **5** due to its poor solubility in CH<sub>3</sub>CN) shows that the <sup>1</sup>MLCT bands red-shift in the less polar solvent CH<sub>2</sub>Cl<sub>2</sub> in comparison to the shifts in CH<sub>3</sub>CN or acetone (Figure 3), suggesting that the dipole moment of the ground state is larger than that of the excited state.<sup>8a,17</sup> This is in line with what is found for platinum terpyridyl complexes.<sup>3b</sup> When the absorption spectra of complexes **1** and **2** and those of **3** and **4** are compared, it is found that there is no significant change within each pair of complexes. This indicates that the different counteranions exhibit a negligible effect on the electronic absorption spectra of these platinum(II) 2,4-di(2'-pyridyl)-6-(*p*-tolyl)-1,3,5-triazine complexes.

**Emission.** Complexes **2–5** exhibit weak emission at room temperature in fluid solutions, while complex **1** shows no detectable emission in degassed acetonitrile solution. When excited at 325 nm, both **2** and **5** emit at 460 nm in degassed acetonitrile solution (shown in Figure 4), and the emission lifetime is too short to be measured using our instrument, which has a time resolution of 5 ns. In comparison to the <sup>3</sup>MLCT emission of the reported platinum(II) 4'-tolylterpyridyl chloride and acetylide complexes,<sup>3c,d,8a</sup> the emission bands at 460 nm for **2** and **5** are blue-shifted  $\sim 90$  and  $\sim 140$  nm, respectively, and the lifetime of the 460 nm band is much shorter than that of the <sup>3</sup>MLCT band of their corresponding 4'-tolylterpyridyl platinum(II) complexes, which are tens of nanoseconds to hundreds of nanoseconds, respectively. Therefore, the 460 nm emission band must not originate from the <sup>3</sup>MLCT excited state. It is very likely that this emission arises from the ligand <sup>1</sup> $\pi, \pi^*$  excited state, considering the fact that the 325 nm excitation is located at the <sup>1</sup> $\pi, \pi^*$  absorption band of the ligand. In order to reveal the origin of this emission band at 460 nm, the excitation

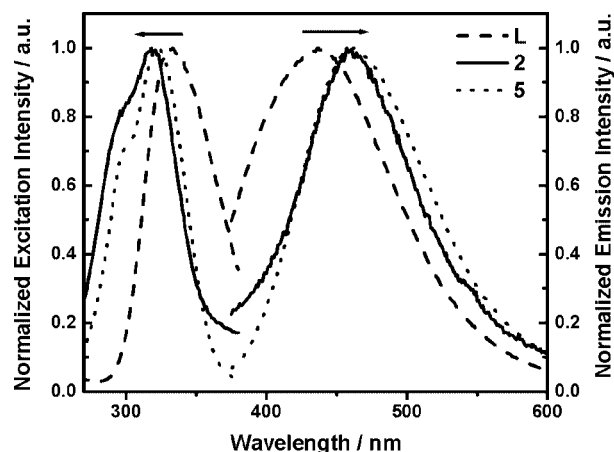


**Figure 4.** Normalized emission and excitation spectra of ligand **L** and complexes **2** and **5** in degassed acetonitrile solutions at a concentration of  $\sim 2.1 \times 10^{-5}$  M. The excitation wavelength is 325 nm for the emission measurement. The excitation spectra were monitored at the corresponding emission band maximum.

spectra of **2** and **5** monitored at an emission wavelength of 460 nm were measured. In addition, the emission of the ligand **L** upon excitation at 325 nm was monitored. As displayed in Figure 4, the emission bands at 460 nm for **2** and **5** are quite similar to that of **L**, with only an approximately 20 nm red shift. This red shift could be attributed to the reduced electron density of the terdentate ligand in the platinum complexes, which would decrease the energy of the ligand  $\pi^*$  orbital and thus induce the red shift. The attribution of the 460 nm emission band to the <sup>1</sup> $\pi, \pi^*$  excited-state is further supported by the excitation spectra measurement. When monitored at 460 nm, the excitation bands of **2** and **5** appear at ca. 318 nm, while the excitation band of **L** occurs at 332 nm. Both of them are located at the ligand <sup>1</sup> $\pi, \pi^*$  absorption band. Therefore, we conclude that the 460 nm emission indeed arises from the ligand <sup>1</sup> $\pi, \pi^*$  excited state.

In addition, the emission band at 460 nm for **2** and **5** shows concentration dependence. As shown in Figure 5 for complex **2**, when the concentration increases from  $4.0 \times 10^{-6}$  to  $2.1 \times 10^{-5}$  M, the emission peak red-shifts and the emission intensity increases. Above  $2.1 \times 10^{-5}$  M, the emission intensity decreases. For complex **5** (Figure 6), a similar trend was observed. Considering the significant ground-state absorption of **2** and **5** around 450 nm, the red shift and decreased intensity of the emission band at higher concentrations could possibly be attributed to an inner-filter effect. On the other hand, either ground-state aggregation or self-quenching can contribute to a decrease in the emission intensity. The attribution to ground-state aggregation could be excluded on the basis of the fact that no ground-state aggregation was observed from UV–vis measurement at the same concentration range used for the emission measurement. However, the possibility of self-quench-

(17) Aldridge, T. K.; Stacey, E. M.; McMillin, D. R. *Inorg. Chem.* **1994**, *33*, 722.

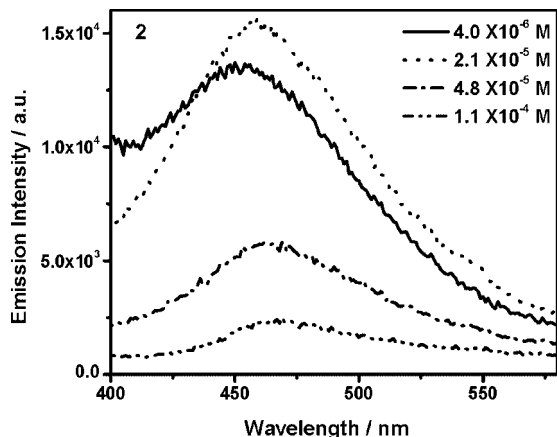


**Figure 5.** Emission spectra of complex **2** at different concentrations in degassed acetonitrile solutions. The excitation wavelength is 325 nm.

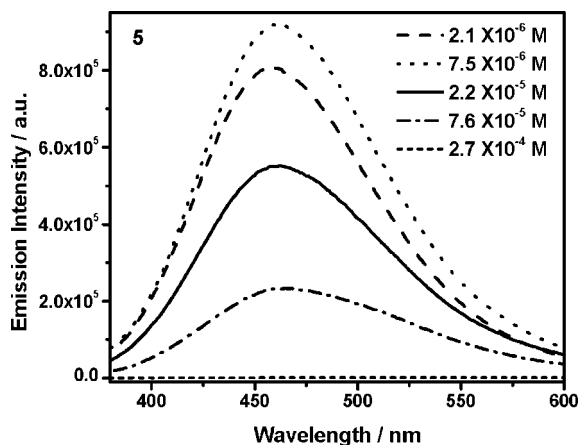


**Figure 6.** Emission spectra of complex **5** at different concentrations in degassed acetonitrile solutions. The excitation wavelength is 325 nm.

ing still could not be ruled out, because of the time-resolution limit of our instrument, which prevents us from obtaining the emission lifetime of the 460 nm emissions.

To verify the contribution from the inner-filter effect, a 5 mm cuvette was used instead of the 1 cm cuvette for the concentration-dependent emission measurement of complex **2**. When the concentration was increased from  $2.0 \times 10^{-5}$  to  $1.0 \times 10^{-4}$  mol L<sup>-1</sup>, no obvious bathochromic shift of the 460 nm emission band was observed. In addition, the quenching of the emission intensity was also reduced. When the 5 mm cuvette was used, the emission intensity decreased to 55% in the  $1.0 \times 10^{-4}$  mol L<sup>-1</sup> solution, in comparison to that in the  $2.0 \times 10^{-5}$  mol L<sup>-1</sup> solution. In contrast, the emission intensity was quenched to 12% when measured in the 1 cm cuvette. Therefore, contribution from the inner-filter effect is clearly evidenced.

For complexes **3** and **4**, the emission band appears at ca. 615 nm with a lifetime of approximately 180 ns at room temperature when excited either within the <sup>1</sup> $\pi,\pi^*$  transition band (i.e., 324 nm) or within the <sup>1</sup>MLCT band (i.e., 453 nm) in CH<sub>2</sub>Cl<sub>2</sub> solutions (shown in Figure 7). In view of the energy and the lifetime of this emission band and with reference to the emission energy of other reported platinum terpyridyl complexes,<sup>3b,8a,14,16</sup> this emission could be assigned to the <sup>3</sup>MLCT excited state. In comparison to the emission of their 4'-tolylterpyridyl analogue, the emission bands of **3** and **4** are red-shifted 34 and 36 nm, respectively.<sup>16</sup> Similar to the red shift of the <sup>1</sup>MLCT absorption

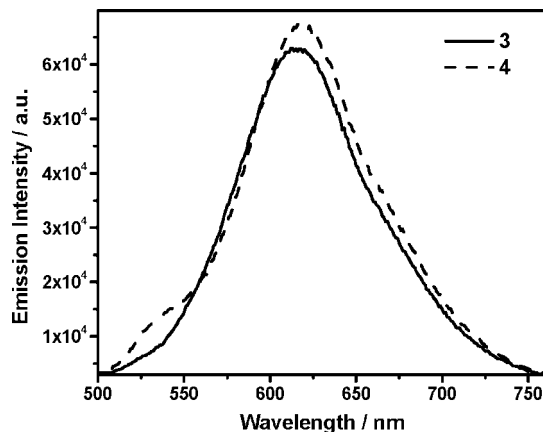


**Figure 7.** Emission spectra of complexes **3** and **4** in degassed CH<sub>2</sub>Cl<sub>2</sub> solutions at a concentration of  $\sim 2.0 \times 10^{-5}$  M. The excitation wavelength is 453 nm.

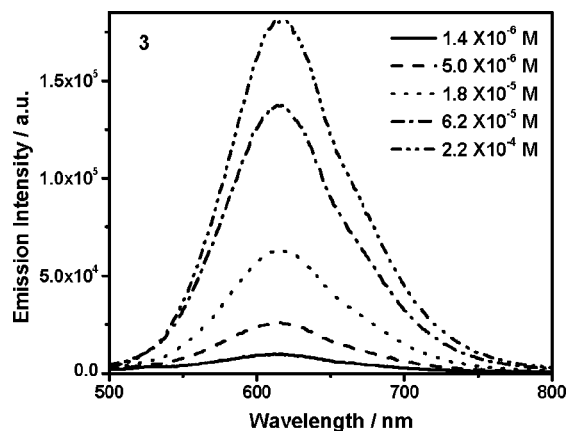


**Figure 8.** Emission spectra of complex **3** at different concentrations in degassed CH<sub>2</sub>Cl<sub>2</sub> solutions. The excitation wavelength is 453 nm.

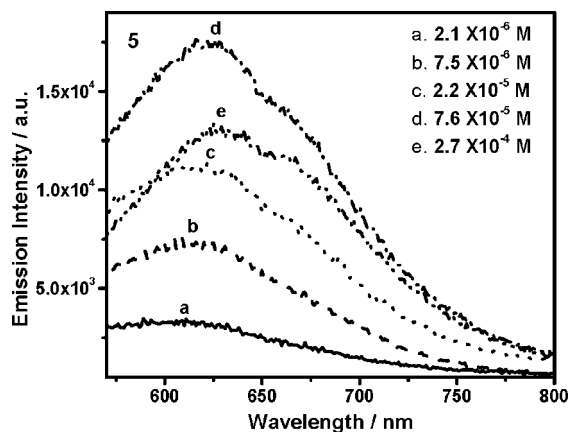


**Figure 9.** Emission spectra of complex **5** at different concentrations in degassed acetonitrile solutions. The excitation wavelength is 479 nm.

band, the red shift of the emission band could also be attributed to the same reason: i.e., the reduced energy of the  $\pi^*$  orbital of the triazine-containing terdentate ligand yields a narrower band gap between the Pt-based HOMO and the terdentate ligand-based LUMO, which in turn decreases the energy of the <sup>3</sup>MLCT excited state. Variation of the counteranion introduces a negligible effect on the emission energies of **3** and **4**. However, the emission quantum yield of **4** is 2.6 times as high as that of

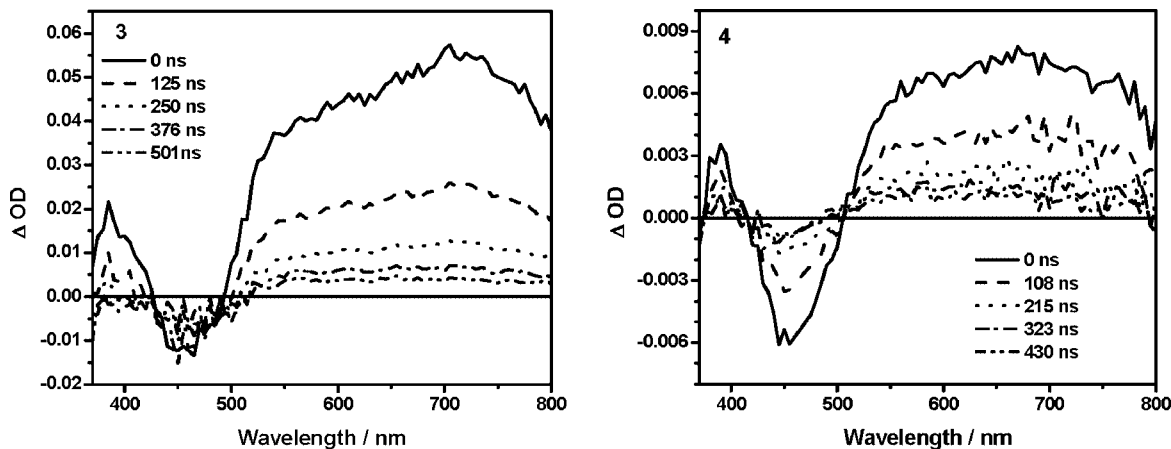


**Figure 10.** Time-resolved triplet transient difference absorption spectra of **3** and **4** in argon-degassed  $\text{CH}_2\text{Cl}_2$  solutions at room temperature following 355 nm excitation. The path length of the cuvette is 1 cm, and the concentration used is  $6.2 \times 10^{-5} \text{ mol L}^{-1}$  ( $A_{355} = 0.888$ ) for **3** and  $3.9 \times 10^{-5} \text{ mol L}^{-1}$  ( $A_{355} = 0.564$ ) for **4**.

**3.** Nevertheless, both complexes exhibit much weaker emission than their platinum(II) terpyridyl analogue, which exhibits  $\Phi_{\text{em}} = 0.25$  in  $\text{CH}_2\text{Cl}_2$ .<sup>16</sup> The reduced emission quantum yields and lifetimes of **3** and **4** should be related to their lower-lying emitting states, which are approximately red-shifted  $\sim 35$  nm compared to that of their platinum(II) terpyridyl analogue (580 nm).<sup>16</sup> According to the energy gap law,<sup>18</sup> when the energy of the emitting state decreases, the probability of radiationless decay increases, which in turn reduces the emission quantum yield and the lifetime.

The concentration-dependent emission of **3** has also been studied. As shown in Figure 8, when the concentration increases, the emission band maximum does not change and the emission intensity continuously increases. This is different from the  $^1\pi,\pi^*$  emission band at 460 nm for **2** and **5**. The difference could simply arise from the quite different ground-state absorptions at 460 and 615 nm that eliminate the inner-filter effect.

When excited at its  $^1\text{MLCT}$  band, for instance 479 nm, complex **5** exhibits a weak emission at ca. 620 nm, which can be assigned to the  $^3\text{MLCT}$  emission and displays a red shift of approximately 20 nm in comparison to its 4'-tolylterpyridyl analogue.<sup>3b</sup> However, the lifetime of this emission was unable to be obtained, due to the very weak emission. The concentration-dependent emission spectra of **5** displayed in Figure 9 shows that, at a concentration of  $2.7 \times 10^{-4} \text{ M}$ , the intensity of the emission decreases, accompanied by a slight red shift. Considering the absence of a significant ground-state absorption around 620 nm and the lack of ground-state aggregation, as evidenced by a concentration-dependent UV-vis study, the decreased emission intensity at high concentration likely originates from self-quenching that is commonly seen in many organometallic complexes, including platinum complexes.<sup>19</sup> For complex **2**, no detectable emission was monitored when it was excited at its  $^1\text{MLCT}$  band, i.e. 406 nm, which is similar to the case for its platinum terpyridyl chloride analogues<sup>6a,8a</sup> and could be ascribed to the quenching of the  $^3\text{MLCT}$  state by the low-lying nonemissive d-d excited state.

**Triplet Transient Difference Absorption (TA) and Non-linear Transmission.** It has been reported that many platinum(II) terpyridyl complexes exhibit a broad-band triplet excited-state absorption in the visible extending to the near-IR region, which usually arises from the  $^3\text{MLCT}$  state.<sup>3</sup> To reveal whether these 2,4-di(2'-pyridyl)-6-(*p*-tolyl)-1,3,5-triazine-based complexes also exhibit triplet excited-state absorption, the triplet transient difference absorption spectra of **1–5** have been measured. Except for **3** and **4**, the other three complexes exhibit no detectable transient absorption, which presumably is associated with their short-lived  $^3\text{MLCT}$  excited state. Figure 10 illustrates the time-resolved triplet transient difference absorption spectra in argon-degassed  $\text{CH}_2\text{Cl}_2$  solutions for **3** and **4**. Similar to the case for their platinum(II) terpyridyl analogue,<sup>3c</sup> both complexes exhibit a broad positive absorption band from 510 to 820 nm, indicating that the excited-state absorptions of **3** and **4** are stronger than those of their ground states. The bleaching bands that occur between 400 and 500 nm are consistent with the  $^1\text{MLCT}$  bands in the UV-vis absorption spectra, suggesting that the transient absorption possibly originates from the  $^3\text{MLCT}$  excited state. This speculation could be supported by the lifetime measurement of the transients, which gives rise to a lifetime of 224 ns monitored at 705 nm for **3** and 177 ns for **4**. In comparison to the similarly short lifetime of the  $^3\text{MLCT}$  emission (183 ns for **3** and 178 ns for **4**), the transient absorption could arise from the same excited state that emits or a state that is in equilibrium with the emitting state. Therefore, the transient absorption could be tentatively assigned to the  $^3\text{MLCT}$  state.

Using the partial saturation method,<sup>13</sup> the triplet extinction coefficients of **3** and **4** at 705 nm and the quantum yields of the triplet excited-state formation have been determined. These values are  $\epsilon_{\text{T}}(705 \text{ nm}) = 3400 \text{ M}^{-1} \text{ cm}^{-1}$  and  $\Phi_{\text{T}} = 0.21$  for **3** and  $\epsilon_{\text{T}}(705 \text{ nm}) = 690 \text{ M}^{-1} \text{ cm}^{-1}$  and  $\Phi_{\text{T}} = 0.83$  for **4**. Unlike the effect of the counteranion on the ground-state absorption, the counteranion affects the triplet excited-state characteristics drastically, which has also been demonstrated by the emission quantum yield discussed in the emission section.

As reported earlier by our group, several platinum terpyridyl based complexes exhibit moderate to strong nonlinear transmission at 532 nm for nanosecond laser pulses, and the nonlinear transmission mainly arises from reverse saturable absorption.<sup>3</sup> The fact that complexes **3** and **4** exhibit a broad positive band from 510 to 820 nm implies that the triplet excited-state

(18) Caspar, J. V.; Meyer, T. J. *J. Phys. Chem.* **1983**, *87*, 952.

(19) (a) Kunkely, H.; Vogler, A. *J. Am. Chem. Soc.* **1990**, *112*, 5625. (b) Wan, K.-T.; Che, C.-M.; Cho, K.-C. *J. Chem. Soc., Dalton Trans.* **1991**, 1077. (c) Hissler, M.; Connick, W. B.; Geiger, D. K.; McGarrah, J. E.; Lipa, D.; Lachicotte, R. J.; Eisenberg, R. *Inorg. Chem.* **2000**, *39*, 447. (d) Lai, S.-W.; Chan, M. C.-W.; Cheung, T.-C.; Peng, S.-M.; Che, C.-M. *Inorg. Chem.* **1999**, *38*, 4046.

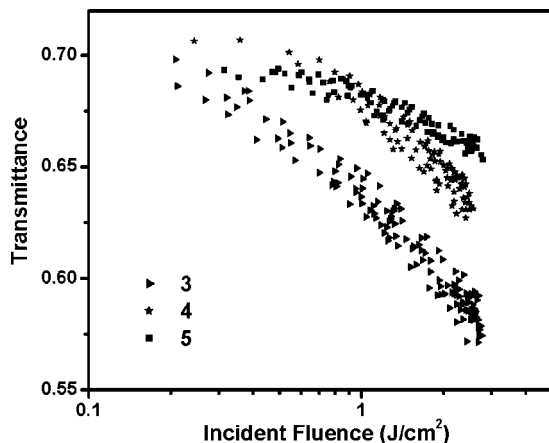


**Figure 11.** Nonlinear transmission curves of **3–5** for 4.1 ns laser pulses at 532 nm in a 2 mm cell. The linear transmission of **3–5** was adjusted to 70%. **3** and **4** were dissolved in  $\text{CH}_2\text{Cl}_2$ , and **5** was dissolved in DMF.

absorption in this spectral range is stronger than that of the ground state. Therefore, reverse saturable absorption and nonlinear transmission are expected to occur in this region. To demonstrate this, nonlinear transmission measurement was conducted for **1–5** at 532 nm using 4.1 ns laser pulses. To compare the degree of nonlinear transmission under the same excitation conditions, all sample solutions except **1** and **2** were adjusted to have a linear transmission of 70% at 532 nm in a 2 mm cuvette. The linear transmission of **1** and **2** was adjusted to 90%, due to the limited solubility of these two samples. It is found that with the increased incident fluence from 0.2 to 3  $\text{J}/\text{cm}^2$ , only complexes **3–5** show a weak transmission drop, among which **3** exhibits the strongest nonlinear transmission (shown in Figure 11). No nonlinear transmission was observed for **1** and **2**. In contrast to their corresponding platinum terpyridyl analogues,<sup>3</sup> the nonlinear transmission behaviors of **3–5** are much weaker. As discovered from other platinum terdentate complexes, the degree of nonlinear transmission is mainly determined by the ratio of the excited-state absorption cross-section ( $\sigma_{\text{ex}}$ ) to that of the ground state ( $\sigma_{\text{g}}$ ). Although **3** and **4** exhibit a broad and moderate triplet transient absorption in the visible to the near-IR region, their ground-state absorption cross-sections at 532 nm, which are  $4.61 \times 10^{-18} \text{ cm}^2$  for **3** and  $5.25 \times 10^{-18} \text{ cm}^2$  for **4**, are almost 1 order of magnitude higher than for the corresponding platinum terpyridyl based complex ( $5.31 \times 10^{-19} \text{ cm}^2$ ).<sup>3c</sup> This would significantly reduce the ratio  $\sigma_{\text{ex}}/\sigma_{\text{g}}$ . As a result, the nonlinear transmission of these complexes drastically decreases. For complex **5**, its ground-state absorption cross-section is even larger ( $1.28 \times 10^{-17} \text{ cm}^2$ ); meanwhile, its triplet excited-state absorption is too weak to be measured. The combination of these two factors results in a much weaker nonlinear transmission.

To rationalize the different nonlinear transmissions of **3** and **4**, it is important to determine the triplet excited-state absorption cross-section at 532 nm. In the transient absorption measurements, if all the molecules pumped out of the ground state either return to the ground state or populate the first triplet excited state within the observation time of the optical density change, the following equation can be used to estimate  $\epsilon_T^{532,13a}$

$$\Delta\text{OD} = (\epsilon_T - \epsilon_g)c_T l \quad (2)$$

where  $\epsilon_T$  and  $\epsilon_g$  are the triplet excited-state and ground-state extinction coefficients, respectively,  $c_T$  is the triplet excited-state concentration, and  $l$  is the optical path length of the sample.

For most platinum(II) complexes, the aforementioned assumption is usually valid due to the heavy-atom effect of platinum, which rapidly depopulates the singlet excited-state to either the ground-state or to the triplet excited state. Therefore, it is valid to use eq 2 to estimate the  $\epsilon_T^{532}$  values for **3** and **4**.

Since the  $\epsilon_T$  value at 705 nm has been measured by the partial saturation method, as discussed in previous paragraphs, the  $\epsilon_g$  value can be deduced from the UV–vis measurement,  $\Delta\text{OD}$  can be obtained from the transient difference absorption spectrum, and the path length for the sample is 1 cm, the triplet excited-state concentration  $c_T$  can thus be estimated. Using this value and the  $\Delta\text{OD}$  and  $\epsilon_g$  values obtained from Figures 10 and 2 at 532 nm, respectively, the  $\epsilon_T$  values at 532 nm are estimated to be  $3130 \text{ M}^{-1} \text{ cm}^{-1}$  for **3** and  $1690 \text{ M}^{-1} \text{ cm}^{-1}$  for **4**. These values correspond to  $\sigma_T$  values of  $1.20 \times 10^{-17} \text{ cm}^2$  for **3** and  $6.47 \times 10^{-18} \text{ cm}^2$  for **4** using the conversion equation  $\sigma = 2303\epsilon/N_A$ , where  $N_A$  is Avogadro's constant. When these values are compared to the ground-state absorption cross-sections at 532 nm, which are  $4.61 \times 10^{-18} \text{ cm}^2$  for **3** and  $5.25 \times 10^{-18} \text{ cm}^2$  for **4**, the ratios  $\sigma_T/\sigma_g$  are found to be 2.60 for **3** and 1.23 for **4**. Although there could be some extent of inaccuracy in the determination of the  $\epsilon_T$  values due to the assumed conditions, the ratio  $\sigma_T/\sigma_g$  for **3** is obviously larger than that for **4**. This probably is the major reason that accounts for its stronger nonlinear transmission at 532 nm in comparison to that of **4**.

## Conclusion

The newly synthesized platinum(II) complexes based on the 2,4-di(2'-pyridyl)-6-(*p*-tolyl)-1,3,5-triazine ligand exhibit bathochromic shifts in their UV–vis absorption spectra and their <sup>3</sup>MLCT emission spectra, which is the result of the electron deficiency of the triazine ring and the extension of the  $\pi$  conjugation between the terdentate ligand and the 6-(*p*-tolyl) substituent due to the increased coplanarity between the ligand and the substituent. However, both the emission efficiency and the lifetime of the emission are significantly reduced compared to those of their corresponding platinum(II) terpyridyl complexes. Complexes **3** and **4** exhibit broad, moderate triplet excited-state absorptions from 510 to 820 nm. However, due to their increased ground-state absorption at 532 nm, their nonlinear transmission for nanosecond laser pulses is significantly reduced. In addition, it has been found that the counter-anion plays a negligible role in the singlet MLCT state but exhibits a drastic effect on the triplet MLCT state, as demonstrated by the emission efficiency, the triplet extinction coefficient, and the triplet quantum yield of **3** and **4**. It also affects the relative nonlinear transmission of these two complexes.

**Acknowledgment** is made to the National Science Foundation (CAREER No. CHE-0449598) and Army Research Laboratory (No. W911NF-06-2-0032) for support. We are also grateful to the North Dakota State EPSCoR (ND EPSCoR Instrumentation Award) for support.

OM701285C